THE JOURNAL OF PHYSICAL CHEMISTRY B

Article

pubs.acs.org/JPCB

Ligand Binding Studied by 2D IR Spectroscopy Using the Azidohomoalanine Label

Robbert Bloem,[†] Klemens Koziol,[†] Steven A. Waldauer,[†] Brigitte Buchli,[†] Reto Walser,[†] Brighton Samatanga,[‡,§] Ilian Jelesarov,[‡] and Peter Hamm*[,†]

[†]Institute of Physical Chemistry, University of Zurich, Zurich 8057, Switzerland

[‡]Department of Biochemistry, University of Zurich, Zurich 8057, Switzerland

[§]Institute of Molecular Biology and Biophysics, ETH Zurich, Zurich 8093, Switzerland

ABSTRACT: We explore the capability of the azidohomoalanine (Aha) as a vibrational label for 2D IR spectroscopy to study the binding of the target peptide to the PDZ2 domain. The Aha label responds sensitively to its local environment and its peak extinction coefficient of 350−400 M^{-1} cm^{-1} is high enough to routinely measure it in the low millimolar concentration regime. The central frequency, inhomogeneous width and spectral diffusion times deduced from the 2D IR line shapes of the Aha label at various positions in the peptide sequence is discussed in relationship to the known X-ray structure of the peptide bound to the PDZ2 domain. The results suggest that the Aha label introduces only a small perturbation to the overall structure of the peptide in the binding pocket. Finally, Aha is a methionine analog that can be incorporated also into larger proteins at essentially any position using protein expression. Altogether, Aha thus fulfills the requirements a versatile label should have for studies of protein structure and dynamics by 2D IR spectroscopy.

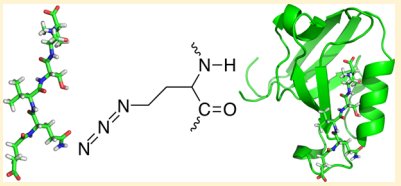

INTRODUCTION

In recent years, it has been shown that two-dimensional infrared (2D IR) spectroscopy is a powerful method to study the structural dynamics of a wide variety of biomolecular systems with very high time resolution.[1] It has been used to study peptide dynamics,[2,3] peptide folding and unfolding,[4,5] protein aggregation[6] and ligand binding.[7] 2D IR spectroscopy is particularly well suited as a companion technique to methods like NMR and X-ray crystallography, which give more structural details but have a lower time resolution (for conceptual or technological reasons, respectively).

However, in general infrared spectroscopy of larger biomolecules, i.e., anything larger than even the smallest proteins, lacks site-specific resolution. To obtain site-specific information, a distinctive label at a specific site is needed with an isolated vibrational frequency, either already present in the molecule or explicitly introduced. A "good label" should give a large and distinctive signal, be sensitive to the environment and it should not disturb the system under study itself. An essentially noninvasive technique uses isotope labeling of atoms already present in the molecule; most commonly of the CO group in the peptide backbone (i.e., the amide I mode). The amide I vibration has a large absorption cross section and is sensitive to its environment.[8,9] The $^{13}C^{16}O$ label red shifts the vibrational frequency by 30 cm^{-1},[10] which sometimes is a bit too small to completely separate the labeled group from the broad main amide I band. In this case, a double isotope $^{13}C^{18}O$ label can be used with a larger 60−70 cm^{-1} red shift.[9,11] In some studies, both labels were used simultaneously to observe coupling between two vibrations.[8,12]

However, isotope labeling has its limitations in the case of larger proteins. First, the natural abundance of ^{13}C of 1% will cause a significant fraction of $^{13}C^{16}O$-labeled amide I modes at random positions in addition to the desired one. Second and more severely, the 1550−1600 cm^{-1} region, where isotope labeled amide I vibrations are expected, is often congested with side chain vibrations from some of the amino acids.[13] Small peptides can be designed to avoid these interferences, but in proteins these side chains are often crucial for correct folding and function and can in most cases not be discarded.

A search is therefore going on to find suitable alternative labels in a less congested part of the spectrum, i.e., in the spectral window between 1900 and 2900 cm^{-1}, were only very few exceptional molecular groups have their fundamental vibrations. The water background is comparably low in this range, albeit not zero due to a broad and unstructured combination band of the water bending and librational mode. Changing between H_2O and D_2O, one can to a certain extent tune that background relative to the vibration of the label. The only naturally occurring vibration in this spectral window is that of the −SH group of cysteins.[14] Alternatively, −CD labeling of natural amino acids might be used as noninvasive labels.[15,16] Both these vibrations are, however, very weak, which is why stronger absorbers in unnatural amino acids are also considered, such as metal carbonyls,[17] cyanides,[18,19] phenyl cyanides,[7,19−24] or the azido moiety.[18,21,25−29] We chose azidohomoalanine (Aha, Scheme 1) as a label because its asymmetric stretch vibration has a reasonably high absorption cross section, and because it is a methionine analog that can be incorporated directly into a protein using the Met auxotrophic

Received: September 25, 2012
Revised: October 31, 2012
Published: November 1, 2012

   dx.doi.org/10.1021/jp3095209 | J. Phys. Chem. B 2012, 116, 13705−13712

Scheme 1. Structure of Azidohomoalanine (Aha)

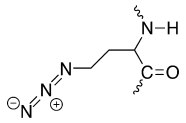

mutants strategy[30] without the need for additional chemical modification after protein expression.[31]

The Aha label has been shown to respond sensitively to its environment.[26,28,29] For example, Raleigh and co-workers have demonstrated a 5−20 cm^{-1} blue shift upon unfolding of an Aha labeled protein.[32] More specifically, a computational study suggested that the angle of hydrogen bonds to the azido group determines the frequency shift which can be as large as 20 cm^{-1}.[33] These characteristics have generated interest in the 2D IR community, such as by the Zanni group[34] and the Bredenbeck group.[35]

In this paper, we explore the potential of the Aha label for ligand binding studies. To that end, we investigate the binding of the target C-terminal peptide from the guanine nucleotide exchange factor RA-GEF-2 ligand (sequence RWADSEADE-NEQVSAV) to the second PDZ domain (PDZ2) of the human protein tyrosine phosphatase 1E (hPTP1E). PDZ domains are found in a wide variety of proteins and act as protein−protein interaction domains that bind to the C-terminus of their target protein. These interactions play an important role in signal transduction[36] and allosteric regulation.[37−39] To study the binding of the peptide to the protein, we labeled an assortment of residues in the peptide. Counting the residues of the peptide from the C-terminus, starting with 0 and counting down, we mutated the peptide at the following positions: Val(−0)Aha, a hydrophobic anchoring point; Ala(−1)Aha and Val(−3)Aha, two sites that are solvent exposed; and Glu(−5)Aha.[40] Ser(−2) and Gln(−4) are hydrogen bonded to the protein through their side chains[40] and were not mutated because this would destabilize binding too much. Using measures deduced from 2D IR lineshapes of the various mutants, we can map out the structure of the peptide bound to PDZ2 in great detail, in full agreement with the known X-ray structure of the ligand-bound form of the protein.[41] In a similar experiment, Fayer and co-workers studied the binding of the S-peptide to the S-protein to form ribonuclease S using cyanophenylalanine as label.[7]

MATERIAL AND METHODS

Sample Preparation. Two variants of the PDZ2 domain from the human phosphatase hPTP1E were used in this work (Table 1). The wild type sequence PDZ2WT was synthesized and cloned into a pET30a vector (EZBiolab, Carmel, IN). The mutation in PDZ2Y36W was introduced by site-directed mutagenesis (QuikChange, Stratagene, La Jolla, CA). Both PDZ2 variants were expressed in *Escherichia coli* BL21(DE3) and purified from inclusion bodies. An N-terminal hexahistidine tag was used for purification with a HisPrep column (GE Healthcare, Life Sciences) in 20 mM Tris HCl, 6 M guanidinium chloride, and 10 mM imidazole at pH 8.0; the protein was eluted with an imidazole gradient. EDTA (40 mM, from a 400 mM stock solution in 100 mM Tris HCl, pH 8) was added to the eluted protein to remove residual nickel bound to the His tag. After incubation at 4 °C for at least 12 h, the protein was refolded using a HiPrep desalting column (GE Healthcare, Life Sciences). PDZ2WT was refolded into 50 mM Tris HCl, pH 8.5, the His tag was removed by a HRV 3C protease digest at 4 °C for 12 h (1 mg of protease:50 mg of protein). The digested protein was separated from the free His tag, uncleaved protein, and protease by an additional HisPrep chromatography step. The buffer was then changed to 50 mM sodium phosphate, 150 mM NaCl, pH 6.8 by desalting using a HiPrep column (this buffer was used for all ITC measurements; for the IR measurements, the same buffer was lyophilized and resuspended in D_2O). The variant PDZ2Y36W was directly refolded into the buffer, and the His tag was not removed. We found no differences between the two variants of the protein in the dissociation constant (Table 2), center frequency of the Aha vibration, or its 2D IR line shape. The latter has been verified for both Ala(−1)Aha and Val(−3)Aha, where measurements have been done with both variants of the protein.

Table 1. Amino Acid Sequences of the Two Variants of the PDZ2 Domain from the Human Phosphatase hPTP1E[a,b]

Protein	Sequence
PDZ2WT	**MHHHHHHDDD DKLEVLFQ'G** PKPGDIFEVE LAKNDNSLGI SVTGGVNTSV RHGGIYVKAV IPQGAAESDG RIHKGDRVLA VNGVSLEGAT HKQAVETLRN TGQVVHLLLE KGQSPT
PDZ2Y36W	**MHHHHHHDDD DK** PKPGDIFEVE LAKNDNSLGI SVTGGVNTSV RHGGI**W**VKAV IPQGAAESDG RIHKGDRVLA VNGVSLEGAT HKQAVETLRN TGQVVHLLLE KGQSPT

[a]Mutations relative to wild type and N-terminal hexahistidine tag with protease cleavage site are in bold. [b]The apostrophe indicates the HRV 3C protease cleavage site.

Table 2. Dissociation Constants K_d of the Wild Type Peptide (Taken from Refs 40 and 41) and the Mutants Used in This Study[a]

peptide	protein	K_d (μM)
WT (15 residues)[40]		5.2
WT (8 residues)[41]		10
WT	Y36W	7.0
WT	WT	7.5
Val(−0)Aha	WT	90
Ala(−1)Aha	Y36W	3.3
Val(−3)Aha	Y36W	58
Glu(−5)Aha	Y36W	15

[a]The error in K_d value of these measurements is typically ±9%.[40]

The RA-GEF-2 sequence was modified to include a Trp for concentration determination, and an Arg for better solubility, resulting in the sequence RWADSEADENEQVSAV. In that sequence, positions 0, −1, −3, and −5 were mutated to Aha, one at a time. Peptides either were synthesized by GL Biochem Ltd. Shanghai or were generated in-house with a CEM Liberty1 peptide synthesizer (Matthews, NC, U.S.A.), using solid-phase peptide synthesis and standard 9-fluorenylmethoxycarbonyl (FMOC) chemistry. The peptides from GL Biochem Ltd. were acetylated at the N-terminus; the ones made in-house were not. The purity of proteins and peptides was confirmed by SDS-PAGE and/or mass spectrometry.

ITC Measurements. For each mutant peptide, the dissociation constant K_d was determined using isothermal titration calorimetry (ITC, Table 2). Measurements were performed on a VP-ITC instrument (GE Healthcare) as described earlier.[40] In short, the sample cell (1.4 mL) was loaded with 70−80 μM of buffered protein solution into which

7−10 μL of peptide solution of about 1.0 mM was injected until saturation. The stirring speed was 300 rpm and experiments were performed at 25 °C. Raw data were processed using the MicroCal analysis software package according to a 1:1 binding model.

IR Measurements. The FTIR spectra were measured using a Bruker Tensor 27 FTIR spectrometer equipped with a MCT detector. The 2D IR measurements were performed on an improved version of the home-built, actively phase-stabilized 2D IR photon echo setup, described previously in refs 9, 42, and 43. In short, an IR pulse (2.2 μJ, 2100 cm^{-1}, 180 cm^{-1} fwhm, ∼100 fs) generated by a Ti:S pumped OPA was split into three equally strong pulses to excite the sample and one weak pulse, the local oscillator (LO). The third pulse was phase cycled by means of a photo elastic modulator to double the signal and at the same time remove scattering.[44] The third-order polarization emitted in the phase matching direction was combined interferometrically with the local oscillator. The two outputs were dispersed in a monochromator (Horiba Jobin Yvon, Triax 190) and imaged onto 2 × 32 MCT array detector (Infrared Associates) and the two signals were subtracted to retrieve the third-order signal. Purely absorptive 2D IR spectra were obtained by adding the rephasing and nonrephasing signals, which were obtained by interchanging the time ordering of the first two pulses. Phasing of the spectra was done using the method described by Backus et al.[45] The data were sampled up to 1.9 ps, giving a 8.9 cm^{-1} resolution after zero padding. The resolution of the spectrometer was 7.4 cm^{-1}.

Compared to our previous work,[9,42,43] improvements have been made to the setup to reach higher sensitivity. First, the repetition rate of the laser system was increased from 1 to 9 kHz. Second, the balanced detection was changed from a beamsplitter to a polarizer based arrangement,[46] which is easier to maintain and use, as it is wavelength independent and intrinsically phase stable because the signal and LO follow the same path. Third, the measurement used a fast scanning technique, where the stages are moving throughout the measurement, to take advantage of the intensity correlation between successive pulses.[47] The recorded data were binned every 2.11 fs. The maximum speed of the motors was 4 shots per bin, which puts it in the slow range of the fast scanning method described in ref 47. Finally, the solvent contribution in the spectra was background subtracted, where two syringe pumps alternately injected either sample or solvent into the measurement cuvette. This was repeated several times between individual scans.

For measurements with only peptide, the lyophilized peptide was resuspended in buffered D_2O. For measurements with protein and peptide, the protein was lyophilized from the buffered solution and resuspended in D_2O and lyophilized peptide was added. Concentrations of peptide and protein were chosen so that at least 90% of the peptide was bound, as deduced from their dissociation constants (Table 2). The peptide concentration was in the range 1.3−6.0 mM and the protein concentration in the range 1.6−7.0 mM. The concentrations of peptides and proteins were measured using the absorption at 280 nm using UV/vis. The samples were filtered before the measurement. The samples were placed into a CaF_2 cuvette of 25 μm thickness in the 2D IR experiments and 57 μm thickness in the FTIR experiments. All measurements were performed at room temperature (20−21 °C).

EXPERIMENTAL RESULTS

Extinction Coefficient of Aha. There has been some confusion in the literature, where the extinction coefficient of Aha is concerned.[18,25,26,32] We therefore start with linear FTIR spectroscopy to provide a solid value for the extinction coefficient, because it is a crucial parameter determining the usefulness of the Aha label. FTIR spectra of three different types of Aha samples have been measured (Figure 1a): Aha

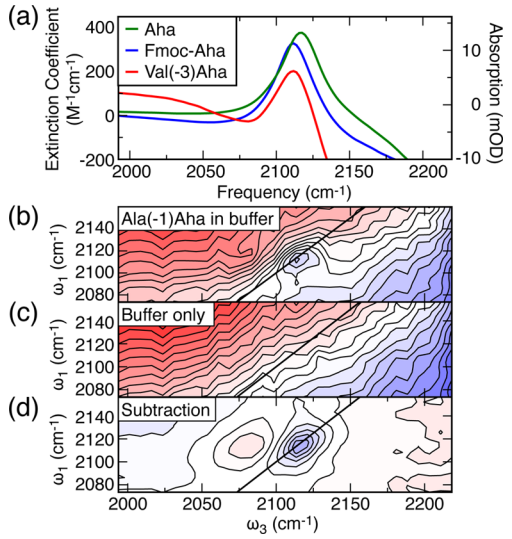

Figure 1. (a) Extinction coefficient of Aha as free amino acid (green), Fmoc-Aha (blue), and Val(−3)Aha (red). The extinction coefficient has been deduced from the measured absorbance by dividing through the concentration (6.3 mM) and the path length of the IR cuvette (57 μm). The buffer background has been subtracted. 2D IR spectra of (b) Ala(−1)Aha with buffer, (c) buffer only, and (d) Ala(−1)Aha with the buffer background subtracted. The concentration of Ala(−1)Aha was 2.7 mM, the waiting time 300 fs. The plots are on the same scale.

incorporated in the peptide (Val(−3)Aha); protected Fmoc-Aha; Aha as free amino acid. In all cases, the Aha peak sits on a significant background, despite the fact that the buffer background has been subtracted. The vibrational frequency of Aha is in the wing of the strong OD-stretching band of the solvent water, which in turn changes quite significantly with the addition of solutes, which is why the background subtraction with the buffer is not perfect. Nonetheless, we find for the center frequency of Aha 2118 cm^{-1}, and 2112 cm^{-1} for both peptide-Aha and Fmoc-Aha. The extinction coefficients of all variants are in the same range 350−400 M^{-1} cm^{-1}.

This value is comparable to those of the closely related azidoalanine (ε = 414 M^{-1} cm^{-1})[18] and azido-NAD^+ (ε = 250 M^{-1} cm^{-1}).[26] On the other hand, our finding differs from ε = 1570 M^{-1} cm^{-1} Gai and co-workers[25] estimated on the basis of data from Raleigh and co-workers.[32] The extinction coefficient of Aha is significantly smaller than that of the azide ion (ε = 2500 M^{-1} cm^{-1}).[43] The latter has strong partial charges (i.e., $N^-{=}N^+{=}N^-$) and hence a very large transition dipole moment for the asymmetric stretch vibration, whereas some of these partial charges are removed due to the covalent bond in the azido group (i.e., essentially $-C{-}N{=}N^+{=}N^-$). Nevertheless, Aha still has a moderately strong extinction coefficient, which is larger than that of most of the alternative unnatural amino acids discussed in the introduction. For example, cyano-alanine has an extinction coefficient of 32 M^{-1}

dx.doi.org/10.1021/jp3095209 | J. Phys. Chem. B 2012, 116, 13705−13712

cm^{-1},[18] resulting in a 100 times smaller 2D IR signal, because the 2D IR response scales quadratically with the extinction coefficient. The extinction coefficient of Aha is weaker than that of the amide I vibration (720 M^{-1} cm^{-1})[18] by only a factor 2; hence it requires only a factor of 4 better signal-to-noise.

Background Suppression. Like the FTIR spectra, the 2D IR signal sits on a significant solvent background. Figure 1b shows the 2D IR spectrum of 2.7 mM unbound Ala(−1)Aha in buffer. One Aha peak can just be distinguished from the background. To remove the background, we separately measured a spectrum with only the buffer (Figure 1c). After subtraction of the buffer spectrum, we obtained the spectrum of Ala(−1)Aha shown in Figure 1d, which clearly shows the pair of peaks that are no longer distorted by the background. The buffer spectrum is sensitive to the alignment of the setup due to effects such as thermal lensing. To eliminate these alignment effects during the background subtraction, sample and buffer were repeatedly exchanged in a flow cell with the help of an automated syringe pump system. Neither the flow cell nor any alignment of the laser beams was modified in any way during that procedure. The number of exchanges between sample and buffer differed per measurement but was usually in the range 5−15. The spectra shown in Figure 1b,c were both measured 10 times, which together took 2.5 h.

The procedure of alternately measuring a sample and a background is common in FTIR spectroscopy and was indeed also used to collect the FTIR spectra of Figure 1a. Even though the procedure is the same, the result of the background subtraction for the 2D IR spectra is better than that for the FTIR spectra. This is a useful side effect of the quadratic scaling of the 2D IR response with the extinction coefficient. The concentration of D_2O is 4 orders of magnitude higher than that of the peptide samples, but the extinction coefficient is 2 orders of magnitude lower. In FTIR, the Aha signal is small compared to the solvent background, making it sensitive to small changes of the solvent signal. In 2D IR, the signal size of Aha and solvent is comparable, making it less sensitive to small changes of the solvent signal. Indeed, the 2D IR spectrum of Figure 1d does not show the slope that is present in the FTIR spectra (Figure 1a).

2D IR Spectroscopy. In the 2D IR measurements, we studied how the azido vibration of Aha is influenced by its environment. It is well established (mostly in the context of the amide I vibration) that the vibrational frequency of such local reporter groups reports on their electrostatic environment. In particular, hydrogen bonds have a strong effect. In the case of the azido group, it has been suggested on the basis of quantum chemistry calculations that water forms hydrogen bonds predominantly to the inner and outer nitrogen atoms of the azido group and that the frequency shift can be a sensitive measure of the geometrical arrangement of these hydrogen bonds.[33] Principally speaking, the frequency position could be measured with FTIR (1D IR) spectroscopy, but 2D IR spectroscopy has much more to offer. First, the quadratic scaling of the 2D IR response on the extinction coefficient discussed above helps tremendously to suppress solvent backgrounds. Second, from a more conceptual point of view, the 2D IR line shape contains additional information not present in FTIR spectra, as we will discuss below.

Figure 2 shows selected 2D IR spectra of mutated peptides, both bound to PDZ2 (blue contours) or unbound (red contours), which are overlaid to facilitate the comparison. In the first case, the concentrations of the peptide and the protein

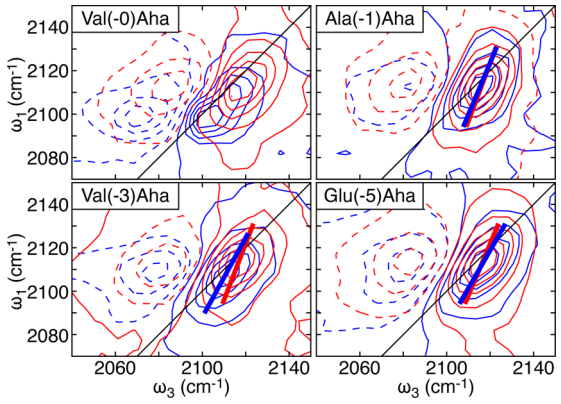

Figure 2. 2D IR spectra of various mutants of the peptide bound to PDZ2 (blue) or unbound (red) at a waiting time of 300 fs. Solid contour lines represent the 0−1 peak, dotted contour lines the 1−2 peak. The thick solid line shows the tilt of the 0−1 peak.

were chosen such that at least 90% of the peptide was bound, as deduced from the corresponding dissociation constant (Table 2). 2D IR spectra always come as a pair of peaks for each vibration, i.e., the 0−1 peak between the vibrational ground and first excited state (bleach and stimulated emission, solid contours) and the 1−2 peak, which is related to excited state absorption (dashed contours). Both peaks are displaced with respect to each other along the ω_3 axis due to the oscillator's anharmonicity, have opposite signs, and partially overlap. The 0−1 peak is therefore distorted in the ω_3 direction, which is why the center frequency we report is read off along the ω_1 axis. To that end, we averaged cuts along the ω_1 direction for two values of ω_3 around the peak and fitted the result with a Lorentzian function.

Bound Val(−3)Aha is clearly red-shifted compared to the unbound peptide by about 7 cm^{-1}. Bound Val(−0)Aha splits into two peaks, separated by 10 cm^{-1}, both of which are red-shifted compared to the unbound peptide. On the other hand, Ala(−1)Aha and Glu(−5)Aha do not show any measurable frequency shift upon binding. The center frequencies of the various samples are compiled in Figure 3b. Some of the samples have been measured more than once, in which case the spread of points gives an idea of the error in these experiments. In addition to the frequency shift of Val(−3)Aha between the

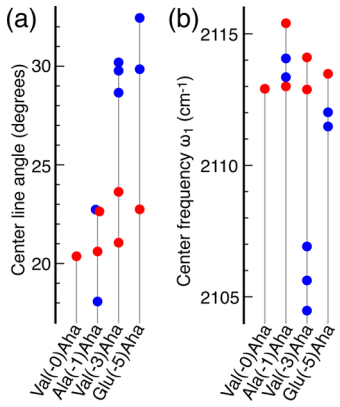

Figure 3. Tilt angle measured at a waiting time of 300 fs (a) and center frequency (b) of all mutants of the peptide, either bound to PDZ2 (blue) or unbound (red). The dots represent individual measurements.

dx.doi.org/10.1021/jp3095209 | J. Phys. Chem. B 2012, 116, 13705−13712

bound and unbound form, Figure 3b also shows that the vibrational frequencies of all mutants of the peptides lie within 3 cm^{-1} when they are not bound. The range of 2113−2116 cm^{-1} agrees well with the FTIR results (Figure 1) and the 2112−2113 cm^{-1} center frequency Raleigh and co-workers found for an unfolded protein with an Aha label.[32]

Analyzing the line shape of a 2D IR peak, we can also study the inhomogeneity and spectral diffusion of a vibrational band. That is, the Aha label will sit in a different local environment for each individual protein in the ensemble, giving rise to a different frequency shift and thus an inhomogeneous broadening of the IR absorption band. In 2D IR spectroscopy, a spectrum is first measured along the ω_1 axis, the system is given time to evolve during a waiting (population) time t_2, and the spectrum is then measured a second time along the ω_3 axis. The resulting 2D IR spectrum therefore reveals the correlation between the two frequency measurements. When the waiting time is short compared to the correlation time of the fluctuations of the system, the motion of the molecule is "frozen", the two frequencies are correlated and the peak will be elongated along the diagonal (Figure 4c, left). When the waiting time is increased, the correlation gets lost because the local environment around a given Aha label is not static, and the tilt of the 2D IR line shape decreases (Figure 4c, right). In other words, on short enough time scales, the spectrum is that of an inhomogeneously broadened ensemble, which changes into a homogeneous ensemble with increasing waiting time. This process is called spectral diffusion.

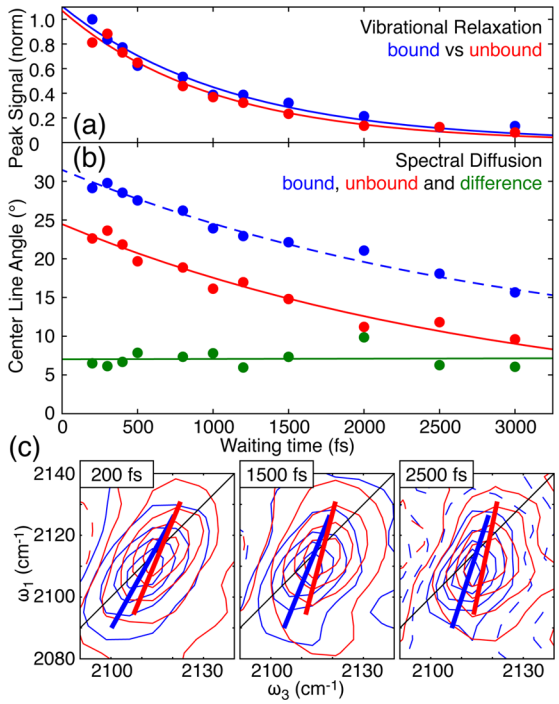

Figure 4. Time resolved measurements with Val(−3)Aha: bound (blue); unbound (red). (a) Decay of the 0−1 peak intensity. The experimental data (dots) are normalized, exponential fits are shown as lines. (b) Time evolution of the center line angle of the 0−1 peak. The dots are experimental data; the fits are discussed in the text. (c) Selected 2D IR spectra for three different waiting times. The data are normalized to the peak intensity of the 0−1 peak, to normalize out the vibrational lifetime decay. Solid contour lines represent the 0−1 peak, dotted contour lines the 1−2 peak. The thick lines are the center line angles.

Several methods have been proposed to quantify the spectral inhomogeneity; the results we show use the center line angle method.[1,48] To determine this tilt, we cut the spectra along different values of ω_1 and fitted these cuts with two Lorentzian functions. The maxima of different cuts were used to fit the tilt angle. Another measure of inhomogeneity is the ellipticity of the 0−1 peak,[49] which we tried as well and yielded qualitatively the same results.

The tilt angles are shown in Figure 2 as thick solid lines, and the results are compiled in Figure 3a. All these data were taken with a waiting time t_2 = 300 fs, which is when pulse overlaps are negligible, and thus represent the instantaneous distribution of local environments around the Aha label. The tilt data divide into two regions. One around 18−24°, where all unbound peptides are found as well as Ala(−1)Aha its bound state, and a region between 28 and 33°, occupied by the bound Val(−3)Aha and Glu(−5)Aha ligands. No tilt angle has been determined for bound Val(−0)Aha because of the overlap of the two peaks.

Plotting the tilt of the 2D IR line shape as a function of waiting time reveals directly the correlation time of the system. We do that in in Figure 4b,c for one representative example, Val(−3)Aha, in both its bound and unbound state. The time window in which spectral diffusion can be measured is limited by the vibrational lifetime of the Aha vibration that diminishes the intensity of the 2D IR signal. A fit of the peak intensity shown in Figure 4a reveals for the vibrational lifetime 1 ps ± 100 fs. We do not find any difference in lifetime between unbound (more solvent exposed) and bound (less solvent exposed) peptide. The lifetime is shorter than that of the azide ion in D_2O (2.4 ps)[50] or 3-azidopyridine in CH_2Cl_2 (4.0 ps).[26] A lifetime of 1.1 ps was also found for the nucleic acid with azido label N_3dU in water.[28]

The selected 2D IR spectra in Figure 4c show how the shape of the 0−1 peak changes from predominantly elongated along the diagonal at 200 fs to a more round and vertically oriented shape at 2.5 ps. Figure 4b shows the time evolution of the center line angle compiled from an extended series of 2D IR spectra. The data do not decay to zero within the time window dictated by the short vibrational lifetime, and we have to be careful when fitting the spectral diffusion time. We fit the tilt angle of the unbound peptide by $\Delta\exp[-t/\tau]$, whereby we implicitly assume that it decays indeed to zero in a single-exponential fashion, and find a correlation time of τ = 3.0 ps. The green data in Figure 4b show the difference of the tilt angle data of bound and unbound peptide, which can very well fit by just a constant c. This result indicates that the only difference between bound and unbound peptide is an inhomogeneous contribution that is quasi-static on the time scale of this experiment. The blue dashed line in Figure 4b is not a fit but shows the function $\Delta\exp[-t/\tau] + c$, where Δ and τ are the values obtained from the fit of the unbound peptide.

DISCUSSION

We have seen in the previous section that the 2D IR band of one label (Val(−0)Aha) splits into a substructure upon binding to the protein, one changes in both its central frequency and inhomogeneous width (Val(−3)Aha), one only in its inhomogeneous width but not the central frequency (Glu(−5)-Aha), and one does not change at all (Ala(−1)Aha). In the following, we will discuss this rich behavior based on the known

dx.doi.org/10.1021/jp3095209 | J. Phys. Chem. B 2012, 116, 13705−13712

X-ray structure of the wild-type peptide bound to PDZ2 shown in Figure 5.[41] As a starting point for the discussion, we

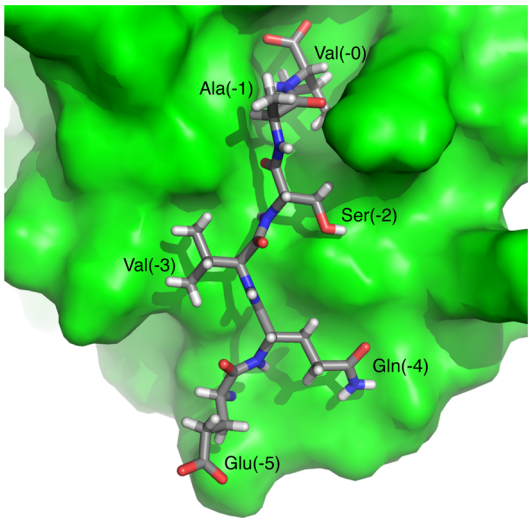

Figure 5. Binding pocket of the protein with the wild type peptide bound (PDB ID 3LNY).[41]

implicitly assume that the orientation of the Aha side chain is essentially the same as that of the corresponding amino acid in the wild type peptide, so we can guess the local environment of the Aha label in the various mutants. This assumption is motivated by the relatively small changes of the dissociation constant (with the one exception of Val(−0)Aha, Table 2), suggesting that the mutant's anchor points are essentially the same. Furthermore, the peptide is stretched into a very extended structure by multiple hydrogen bonds from the peptide backbone as well as the Ser(−2) and Gln(−4) side chains;[40] hence the directions of the other side chains are relatively rigidly defined. However, in detail, the orientation of the Aha side chain might of course deviate from that of the wild type peptide, in particular given the fact that Aha is longer than Ala or Val, for example, and indeed we will see for the case of Val(−0)Aha that the structure is perturbed. At this point it might help that Aha might be considered an "amphiphilic" amino acid with two hydrophobic CH_2 groups and the $-N_3$ as a polar head. As such, regardless whether it replaces an apolar or a polar amino acid it might offer similar binding possibilities to the protein surface as the wild type peptide.

We start with Ala(−1)Aha, which does not show any difference in either frequency or inhomogeneity upon binding to PDZ2. This might be expected because Ala(−1) points toward the solvent (Figure 5), so it is solvent exposed in both the bound and the unbound state. The effect of the presumably more rigid structure of water in the protein solvation layer[51] does not seem to be sufficient to cause any measurable effect on the Aha vibrational properties. This mutant may be regarded as a reference sample because it shows that the constraint imposed by binding to the protein does not affect the azido group. Apparently, the ethylene group between the peptide backbone and the azido chromophore separates the latter sufficiently from the former, so the azido vibration really serves as an isolated probe of its direct environment.

Bound and unbound Val(−3)Aha does show a difference in both center frequency and inhomogeneity. The time-resolved measurements (Figure 4b) show that the difference in the instantaneous inhomogeneity (Figures 2 and 3a) is caused by a contribution that is static on the 2D IR time scale, whereas the fast (3 ps) component is the same for both cases. Moreover, the 7 cm^{-1} frequency shift of bound Val(−3)Aha shows a change in the electrostatic environment of the azido group. We have seen with Ala(−1)Aha that binding per se does not change the spectral properties of the azido group, so they must be the result of a specific contact of the label with the protein. The observations suggest that Val(−3) lies on top of the protein surface (Figure 5), so it interacts with the protein but is solvent exposed as well. This explanation is consistent with a computational study that has shown for a different protein system that only the inner and outer nitrogen participate in hydrogen bonding with water, whereas the partially positively charged middle nitrogen interacts with the protein and is responsible for the slow dynamics.[52] We do not find any slowing down of Aha spectral diffusion within the protein solvation shell as compared to bulk water.

Bound Glu(−5)Aha has a higher tilt angle, indicating a more heterogeneous environment, even though the center frequency is the same as for the unbound peptide. The X-ray structure (Figure 5) would suggest that the Glu(−5) side chain is close to the protein surface. The larger inhomogeneous broadening (which is not observed for Ala(−1)Aha) is again evidence for a specific contact with the protein, whereas the absence of a frequency shift might be the result of a cancelation of different interactions. Quantum chemistry calculations indeed suggest that different hydrogen bond configurations to the azido group may cause frequency shifts in opposite directions.[52]

Val(−0)Aha is a special case because we see two peaks, both shifted relative to the peak of unbound Val(−0)Aha. Although the binding affinity of Val(−0)Aha is the lowest of all mutants, the dissociation constant obtained by the ITC measurements verifies that 95% of the peptide was bound to PDZ2 for the concentrations in this specific experiment. Hence, the double peak reveals that the azido group exists in two distinct conformations in the bound form. In the wild type, Val resides inside a hydrophobic binding pocket. Because Aha is much more polar, it might leave that pocket in one of the two conformations. This might also affect the proper positioning of the C-terminal COO^- group, which is an important anchoring point of the wild type ligand. Testing this hypothesis would require a detailed analysis of the structure using X-ray crystallography, NMR, or molecular dynamics simulations and is beyond the scope of this paper.

■ CONCLUSION

In summary, we have measured 2D IR spectra of a library of peptides in which a single residue has been mutated to the unnatural amino acid Aha. By comparing 2D IR spectra of the Aha label bound to the PDZ2 domain with the unbound case, we can elucidate the change upon binding of the electrostatic environment in the vicinity of the label. The spectral changes we observe for the various mutants are fully consistent with the known X-ray structure of the wild-type peptide bound to the PDZ2 domain. This suggests that the Aha label introduces only a small perturbations to the overall structure of the system, and that its response to the environment is sufficient to use it as a local structural probe. At the same time, the peak extinction coefficient of 350−400 M^{-1} cm^{-1} is high enough to routinely measure Aha in the low millimolar concentration regime. In the present study, the Aha label was incorporated in a small peptide that can be synthesized chemically. However, we reiterate that Aha is a methionine analog that can be incorporated also into

larger proteins at essentially any position using protein expression,[30,31] which we consider to be a strong selling point of that label. Hence, Aha fulfills all requirements a "good label" should have for studies of protein structure and dynamics 2D IR spectroscopy.

2D IR is a more complicated technique than FTIR, but its use pays off in several ways. First it suppresses solvent backgrounds due to the fact that the absorption scales with the absorption coefficient squared. The small change in the line shape of the solvent background absorption distorts the FTIR spectra severely but influences the 2D IR spectra much less. Second, the 2D IR line shape contains extra information not available from FTIR (1D IR) spectroscopy. An illustrative example is Glu(−5)Aha, which does not show any frequency shift upon binding, so from FTIR spectroscopy one could be misled and conclude that it does not interact with the protein. 2D IR spectroscopy, in contrast, clearly shows that it does in fact interact with the protein, as evidenced by the larger inhomogeneity of the absorption line. Finally, 2D IR spectroscopy is intrinsically a fast spectroscopy. In the present case, we can see the ultrafast equilibrium fluctuations of solvation water around the protein. In future work, we plan to photoswitch the ligand[53,54] to study the dissociation event of the ligand with unprecedented structural and time resolution.

AUTHOR INFORMATION

Corresponding Author

*E-mail: phamm@pci.uzh.ch.

Notes

The authors declare no competing financial interest.

ACKNOWLEDGMENTS

We thank Ben Schuler and his group for tremendous help with the protein chemistry. This work has been supported by an ERC advanced investigator grant (DYNALLO) and by the Swiss National Science Foundation (SNF) through the NCCR network MUST.

REFERENCES

(1) Hamm, P.; Zanni, M. T. *Concepts and Methods of 2D Infrared Spectroscopy*, 1st ed.; Cambridge University Press: Cambridge, U.K., 2011.

(2) Kim, Y. S.; Hochstrasser, R. M. *J. Phys. Chem. B* **2009**, *113*, 8231−8251.

(3) Adamczyk, K.; Candelaresi, M.; Robb, K.; Gumiero, A.; Walsh, M. A.; Parker, A. W.; Hoskisson, P. A.; Tucker, N. P.; Hunt, N. T. *Meas. Sci. Technol.* **2012**, *23*, 062001.

(4) Backus, E. H. G.; Bloem, R.; Pfister, R.; Moretto, A.; Crisma, M.; Toniolo, C.; Hamm, P. *J. Phys. Chem. B* **2009**, *113*, 13405−13409.

(5) Bagchi, S.; Thorpe, D. G.; Thorpe, I. F.; Voth, G. A.; Fayer, M. D. *J. Phys. Chem. B* **2010**, *114*, 17187−17193.

(6) Shim, S.-H.; Gupta, R.; Ling, Y. L.; Strasfeld, D. B.; Raleigh, D. P.; Zanni, M. T. *Proc. Natl. Acad. Sci. U. S. A.* **2009**, *106*, 6614−6619.

(7) Bagchi, S.; Boxer, S. G.; Fayer, M. D. *J. Phys. Chem. B* **2012**, *116*, 4034−4042.

(8) Ganim, Z.; Chung, H. S.; Smith, A. W.; DeFlores, L. P.; Jones, K. C.; Tokmakoff, A. *Acc. Chem. Res.* **2008**, *41*, 432−441.

(9) Backus, E. H. G.; Bloem, R.; Donaldson, P. M.; Ihalainen, J. A.; Pfister, R.; Paoli, B.; Caflisch, A.; Hamm, P. *J. Phys. Chem. B* **2010**, *114*, 3735−3740.

(10) Woutersen, S.; Hamm, P. *J. Chem. Phys.* **2001**, *114*, 2727.

(11) Torres, J.; Kukol, A.; Goodman, J. M.; Arkin, I. T. *Biopolymers* **2001**, *59*, 396−401.

(12) Fang, C.; Wang, J.; Kim, Y. S.; Charnley, A. K.; Barber-Armstrong, W.; Smith, A. B.; Decatur, S. M.; Hochstrasser, R. M. *J. Phys. Chem. B* **2004**, *108*, 10415−10427.

(13) Barth, A. *Prog. Biophys. Biophys. Chem.* **2000**, *74*, 141−173.

(14) Kozinski, M.; Garrett-Roe, S.; Hamm, P. *J. Phys. Chem. B* **2008**, *112*, 7645−7650.

(15) Naraharisetty, S. R. G.; Kasyanenko, V. M.; Zimmermann, J.; Thielges, M. C.; Romesberg, F. E.; Rubtsov, I. V. *J. Phys. Chem. B* **2009**, *113*, 4940−4946.

(16) Nydegger, M. W.; Rock, W.; Cheatum, C. M. *Phys. Chem. Chem. Phys.* **2011**, *13*, 6098.

(17) King, J. T.; Arthur, E. J.; Brooks, C. L., III; Kubarych, K. J. *J. Phys. Chem. B* **2012**, *116*, 5604−5611.

(18) Oh, K.-I.; Lee, J.-H.; Joo, C.; Han, H.; Cho, M. *J. Phys. Chem. B* **2008**, *112*, 10352−10357.

(19) Getahun, Z.; Huang, C.-Y.; Wang, T.; De León, B.; DeGrado, W. F.; Gai, F. *J. Am. Chem. Soc.* **2003**, *125*, 405−411.

(20) Watson, M. D.; Gai, X. S.; Gillies, A. T.; Brewer, S. H.; Fenlon, E. E. *J. Phys. Chem. B* **2008**, *112*, 13188−13192.

(21) Silverman, L. N.; Pitzer, M. E.; Ankomah, P. O.; Boxer, S. G.; Fenlon, E. E. *J. Phys. Chem. B* **2007**, *111*, 11611−11613.

(22) Schultz, K. C.; Supekova, L.; Ryu, Y.; Xie, J.; Perera, R.; Schultz, P. G. *Journ. Am. Chem. Soc.* **2006**, *128*, 13984−13985.

(23) Waegele, M. M.; Tucker, M. J.; Gai, F. *Chem. Phys. Lett.* **2009**, *478*, 249−253.

(24) Urbanek, D. C.; Vorobyev, D. Y.; Serrano, A. L.; Gai, F.; Hochstrasser, R. M. *J. Phys. Chem. Lett.* **2010**, *1*, 3311−3315.

(25) Waegele, M. M.; Culik, R. M.; Gai, F. *J. Phys. Chem. Lett.* **2011**, *2*, 2598−2609.

(26) Nydegger, M. W.; Dutta, S.; Cheatum, C. M. *J. Chem. Phys.* **2010**, *133*, 134506.

(27) Ye, S.; Zaitseva, E.; Caltabiano, G.; Schertler, G. F. X.; Sakmar, T. P.; Deupi, X.; Vogel, R. *Nature* **2010**, *464*, 1386−1389.

(28) Tucker, M. J.; Gai, X. S.; Fenlon, E. E.; Brewer, S. H.; Hochstrasser, R. M. *Phys. Chem. Chem. Phys.* **2011**, *13*, 2237−2241.

(29) Wolfshorndl, M. P.; Baskin, R.; Dhawan, I.; Londergan, C. H. *J. Phys. Chem. B* **2012**, *116*, 1172−1179.

(30) Kiick, K.; Saxon, E.; Tirrell, D.; Bertozzi, C. *Proc. Natl. Acad. Sci. U. S. A.* **2002**, *99*, 19.

(31) Jo, H.; Culik, R. M.; Korendovych, I. V.; DeGrado, W. F.; Gai, F. *Biochemistry* **2010**, *49*, 10354−10356.

(32) Taskent-Sezgin, H.; Chung, J.; Banerjee, P. S.; Nagarajan, S.; Dyer, R. B.; Carrico, I.; Raleigh, D. P. *Angew. Chem., Int. Ed.* **2010**, *49*, 7473−7475.

(33) Choi, J.-H.; Oh, K.-I.; Cho, M. *J. Chem. Phys.* **2008**, *129*, 174512.

(34) Mukherjee, Sudipta S.; Zanni, Martin T. 2D IR spectroscopy of azido labeled amino acid as a probe of protein structure. Unpublished results presented at CMDS 2010 Meeting.

(35) Müller-Werkmeister, H. M.; Bredenbeck, J. Artificial amino acids as site-specific probes for ultrafast dynamics in proteins. Unpublished results presented at CMDS 2012 Meeting.

(36) Lee, H.; Zheng, J. *Cell Commun. Signaling* **2010**, *8*, 8.

(37) Fuentes, E.; Der, C.; Lee, A. *J. Mol. Biol.* **2004**, *335*, 1105−1115.

(38) Gianni, S.; Walma, T.; Arcovito, A.; Calosci, N.; Bellelli, A.; Engström, Å.; Travaglini-Allocatelli, C.; Brunori, M.; Jemth, P.; Vuister, G. W. *Structure* **2006**, *14*, 1801−1809.

(39) van den Berk, L. C. J.; Landi, E.; Walma, T.; Vuister, G. W.; Dente, L.; Hendriks, W. J. A. J. *Biochemistry* **2007**, *46*, 13629−13637.

(40) Milev, S.; Bjelic′, S.; Georgiev, O.; Jelesarov, I. *Biochemistry* **2007**, *46*, 1064−1078.

(41) Zhang, J.; Sapienza, P. J.; Ke, H.; Chang, A.; Hengel, S. R.; Wang, H.; Phillips, G. N., Jr.; Lee, A. L. *Biochemistry* **2010**, *49*, 9280−9291.

(42) Volkov, V.; Schanz, R.; Hamm, P. *Opt. Lett.* **2005**, *30*, 2010−2012.

(43) Kozinski, M.; Garrett-Roe, S.; Hamm, P. *Chem. Phys.* **2007**, *341*, 5−10.

(44) Bloem, R.; Garrett-Roe, S.; Strzalka, H.; Hamm, P.; Donaldson, P. *Opt. Express* **2011**, *18*, 27067−27078.

(45) Backus, E. H. G.; Garrett-Roe, S.; Hamm, P. *Opt. Lett.* **2008**, *33*, 2665−2667.
(46) Middleton, C.; Strasfeld, D.; Zanni, M. *Opt. Express* **2009**, *17*, 14526−14533.
(47) Helbing, J.; Hamm, P. *J. Opt. Soc. Am. B* **2011**, *28*, 171−178.
(48) Roberts, S. T.; Loparo, J. J.; Tokmakoff, A. *J. Chem. Phys.* **2006**, *125*, 084502.
(49) Lazonder, K.; Pshenichnikov, M. S.; Wiersma, D. A. *Opt. Lett.* **2006**, *31*, 3354−3356.
(50) Li, M.; Owrutsky, J.; Sarisky, M.; Culver, J. P.; Yodh, A.; Hochstrasser, R. M. *J. Chem. Phys.* **1993**, *98*, 5499.
(51) Zhong, D.; Pal, S. K.; Zewail, A. H. *Chem. Phys. Lett.* **2011**, *503*, 1−11.
(52) Choi, J.-H.; Raleigh, D.; Cho, M. *J. Phys. Chem. Lett.* **2011**, *2*, 2158−2162.
(53) Ihalainen, J. A.; Paoli, B.; Muff, S.; Backus, E. H. G.; Bredenbeck, J.; Woolley, G. A.; Caflisch, A.; Hamm, P. *Proc. Natl. Acad. Sci. U. S. A.* **2008**, *105*, 9588−9593.
(54) Waldauer, S. A.; Hassan, S.; Paoli, B.; Donaldson, P. M.; Pfister, R.; Hamm, P.; Caflisch, A.; Pellarin, R. *J. Phys. Chem. B* **2012**, *116*, 8961−8973.